Coulomb blockade phenomena in ultrathin Langmuir-Blodgett sandwich junctions

1999 J. Phys.: Condens. Matter 11 2993

(http://iopscience.iop.org/0953-8984/11/14/015)

J. Phys.: Condens. Matter **11** (1999) 2993–3002. Printed in the UK PII: S0953-8984(99)97675-0

Coulomb blockade phenomena in ultrathin Langmuir–Blodgett sandwich junctions

M Burghard, C Mueller-Schwanneke, G Philipp and S Roth

Max-Planck-Institut für Festkörperforschung, Heisenbergstrasse 1, D-70569 Stuttgart, Germany

Received 18 September 1998

Abstract. Electrical junctions were fabricated in sandwich configuration from Langmuir–Blodgett (LB) films of two types of material, π-conjugated, peripherally substituted ring systems or a σ-bonded polymer. The sandwich junctions consisted of four to ten monolayers between two micro-structured gold electrodes, corresponding to a nominal film thickness between about 8 and 20 nm. At liquid helium temperature, the current (I)/voltage (V) characteristics generally exhibited smooth exponential behaviour or irregular steps. However, for a small fraction of the LB sandwiches comprising a π-conjugated or σ-bonded compound, regular staircases were observed. It was possible to fit such I/V characteristics with curves calculated on the basis of a Coulomb blockade model. These results are accounted for by the presence of nanometre-sized gold particles formed upon evaporation of the top electrode. Single electron tunnelling is assumed to proceed through double tunnel barrier junctions consisting of a gold island asymmetrically located between the top and bottom electrode.

1. Introduction

Considerable effort was recently devoted to electrically contacting one single nanoparticle or an ordered arrangement of a few quantum-dot-like particles with sizes in the nm range. Examples include metal clusters [1], semiconductor nanocrystallites [2] and molecules [3]. Due to their small size, these systems are promising for the investigation of quantum transport phenomena close to room temperature. This feature is in contrast to lithographically defined structures which usually require temperatures below 4 K in order to suppress thermally induced charge fluctuations [4]. Under specific conditions, the electrical transport behaviour of a quasi-isolated quantum dot coupled to macroscopic electrodes via two tunnelling barriers can reflect the ultrasmall dot capacitance or the spectrum of its discrete energy levels. Single electron tunnelling (SET) phenomena [5] like a Coulomb blockade or Coulomb staircase can be observed, if the charging energy $E_C = e^2/2C$ (where C represents the dot capacitance) of the dot exceeds the thermal energy k_BT and the tunnel resistances are large compared to $R_K = h/e^2$. SET might find application [6] for single-electron transistors, turnstiles or pumps.

Current/voltage (I/V) characteristics of islands in a double barrier tunnel junction have most often been recorded with the aid of a scanning tunnelling microscope (STM). The success of this technique is related to the ease of selecting one of the randomly arranged particles without the need for its controlled adsorption at a specific position on a substrate. In the beginning, STM experiments were performed on metallic nanoparticles prepared by metal evaporation onto a thin insulating layer on an electrode [7]. In the later stage, researchers also used colloidal metal particles [8] and ligand stabilized metal clusters [9] deposited on

0953-8984/99/142993+10$19.50

electrodes covered with an organic or inorganic insulator. Metal islands with a diameter d smaller than 5 nm were shown to display SET effects up to room temperature [10]. Evidence for discrete energy levels in metal nanoparticles was provided by the STM investigation of Dubois *et al* on ligand stabilized platinum clusters [11] ($d \approx 2$ nm). Coulomb blockade was also observed for semiconductor nanoparticles by using an STM tip [12]. In contrast, clear-cut demonstrations of SET effects in molecular systems are rare. An intriguing example is the STM study on isolated C_{60} molecules by Porath and Millo which reflected discrete molecular energy levels [13].

The technological application of the STM technique is, however, restricted by the low stability of the tip/substrate configuration. Therefore, recent investigations have focused on electrical contacts made with lateral electrodes. As an example, Sato and Ahmed reported a Coulomb staircase in transport through a metal particle ($d = 10$ nm) chain [14]. Furthermore, Klein *et al* succeeded in the fabrication of a single-electron transistor from an individual semiconductor nanocrystal ($d = 5.5$ nm) [15].

Compared to STM and in-plane contact studies, much less evidence for SET in (organic) vertical junctions is documented. To close this gap, we started to investigate different Langmuir–Blodgett (LB) films consisting of a few (4–10) monolayers incorporated between two noble metal electrodes. Generally, LB layers could serve as a suitable structural matrix for embedding electrically active units like clusters or large molecules and could further act as tunnelling barriers between these units and the electrodes. Towards this end, we first performed electrical transport studies on the one-component LB films incorporated between two microstructured gold electrodes in a sandwich-like configuration. In the present study, two types of material, π-conjugated molecules and a polymer with saturated σ bonds, were used. Both π-conjugated as well as σ-saturated compounds were investigated to clarify whether the presence of π systems gives rise to a larger conductivity through the molecular film.

2. Experimental section

Gold bottom electrodes were patterned by optical lithography on polished BK7 glass substrates or on silicon wafers with a 1 μm thermal oxide layer. The gold was evaporated with a rate of 0.8 nm s^{-1} onto about 0.5 nm of chromium to a total thickness of between 6 nm and 10 nm. Sufficient conductivity ($R \approx 1$ kΩ at room temperature) of the gold stripes could be confirmed for an electrode thickness down to 6 nm.

Figure 1 displays the chemical structure of the octasubstituted metallophthalocyanine PcPd, the perylene derivative PTCDI-SC5 and the non-conjugated, σ-bonded polymer PolC5F, respectively. PcPd was synthesized by the group of Professor M Hanack (University of Tübingen, Germany). The synthesis of PTCDI-SC5 was carried out as described previously [16], PolC5F was prepared from 1H, 1H, 5H-perfluoro-1-pentanol and poly-(maleicanhydride-co-octadec-1-en) in a procedure similar to that reported by Winter *et al* [17].

The substrates were rendered hydrophobic prior to LB transfer by treatment with a 50% solution of hexamethyldisilazane in chloroform (12 hours at room temperature). LB films were fabricated as recently described for PcPd [18] and PTCDI-SC5 [16]. PolC5F monolayers were compressed on a LAUDA FW1 trough ($T = 15\,^{\circ}$C, target surface pressure $\pi = 25$ mN m^{-1}) and deposited by vertical dipping with a speed of 0.5 mm min^{-1} for both up- and downstroke. An important aspect of the PolC5F monolayers is their preparation on an aqueous subphase containing 5 mg l^{-1} of cysteamine (2-amino-ethanethiol). This thiol binds to the carboxylic acid functions on the PolC5F backbone via acid/base reaction forming a PolC5F–COO^{-} $^{+}NH_3$–CH_2–CH_2–SH salt. The introduction of thiol groups into the polar headgroup region of the PolC5F film was performed in order to provide attachment groups for

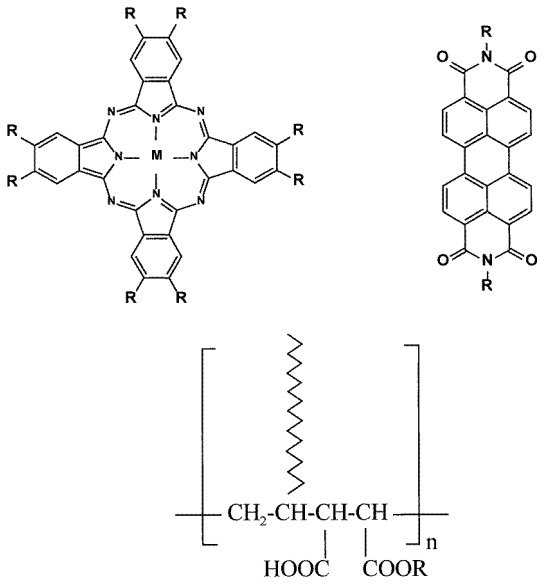

Figure 1. Chemical structure of the octasubstituted palladium phthalocyanine PcPd (top left, M = Pd, R = OC_5H_{11}), the perylene-tetracarboxyldiimide derivative PTCDI-SC5 (top right, R = CH_2–$CH[SC_5H_{11}]_2$) and the σ-bonded amphiphilic polymer PolC5F (bottom, R = $C_5F_8H_3$).

the gold atoms of the top electrode. Earlier studies demonstrated that in this way the number of short circuits can be substantially reduced [19].

The top gold contact was evaporated with an effective rate of 0.004 nm s^{-1} to a thickness of 15 nm using a rotating shutter technique [20]. Contact areas ranged between 30 μm^2 and 2000 μm^2. Electrical measurements were performed in a helium cryostat with a Keithley 617 electrometer and a Keithley 230 voltage source. To check their stability under an electrical field, the contacts were electrically characterized by two successive scans within a given bias range.

3. Results and discussion

3.1. General transport characteristics

The basic transport properties of LB sandwiches consisting of PcPd, PTCDI-SC5 and PolC5F turned out to be similar. In all three of these films, junctions with fewer than four monolayers were apparently short-circuited by gold filaments and exhibited linear I/V curves with a resistance of less than 1 MΩ. According to small angle x-ray reflectivity results [21, 22], four layers correspond to a total LB film thickness of 8.6 nm for PcPd, 6.9 nm for PTCDI-SC5 and 7.1 nm in the case of PolC5F.

On the other hand, if the gold contacts were separated by four or more monolayers a variety of different I/V characteristics was obtained, depending on which junction on the substrate was chosen. In general, I/V curves falling into three different categories were observed at 4.2 K: (a) curves with smooth exponential current increase, (b) curves with at least one abrupt current increase and (c) curves with (multiple) current *steps*. Curves of type (b) are not further considered in this paper. They had been interpreted by resonant tunnelling through molecular orbitals [23] which, however, might be regarded as tentative as long as other explanations like

electromigrative formation or restructuring of metallic filaments cannot definitely be excluded. I/V characteristics of type (c) are discussed in more detail under section 3.2.

Smooth exponential I/V curves of type (a) have also been reported for other types of LB film contacted in sandwich geometry. A number of different transport mechanisms have been invoked to explain such characteristics, including direct tunnelling [24], Fowler–Nordheim tunnelling [25], Schottky emission [26] as well as hopping conduction between defect sites [27]. For a substantial fraction of the present junctions displaying curves of type (a), hopping conduction appears to be the most plausible transport mechanism. This conclusion is drawn from two observations. First, curves of type (a) were more often observed, if thicker (>6 monolayers) LB films were contacted. Electrical transport through such multilayered films is expected to become close to that of the bulk material, and it is reasonable to assume that defect sites are present, especially at the interlayer regions [28]. Secondly, a large fraction of the I/V data followed a linear relationship if the current I was logarithmically plotted against V^{α} with $\alpha = 1/2$ or $1/4$, which is taken as an indication of thermally activated hopping between statistically distributed defect sites [29]. This is exemplified in figure 2 for three different sandwich structures (at room temperature), each consisting of ten monolayers of PcPd. It should, however, be kept in mind that often the assignment to a specific conduction mechanism is not unequivocal, because the (limited number of) data points leads to more or less straight lines for more than one type of 'characteristic' plot.

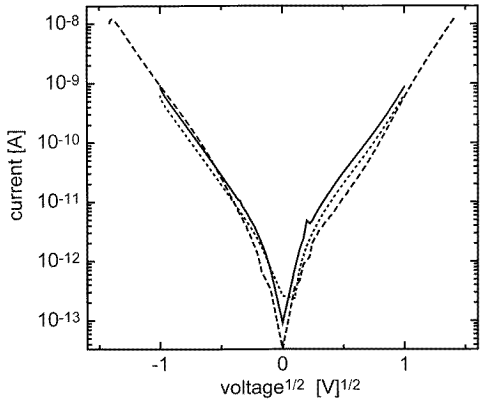

Figure 2. Logarithmic plot of I versus $V^{1/2}$ for three different ten-monolayer PcPd sandwich structures (corresponding to full, dotted and dashed curve, respectively) at room temperature.

As a further observation, thicker films (ten monolayers) of the polymer PolC5F turned out to be more insulating compared to similar films of the π-conjugated compounds. For a considerable fraction of the thicker PolC5F LB films, no current could be detected within the limit of ≈100 fA for voltages up to 3 V. Such a low conductivity was not observed for any of the ten-monolayer PcPd and PTCDI-SC5 contacts. This fact can be explained by the higher mechanical and thermal stability of the polymeric LB film which leads to a larger effective thickness of the PolC5F sandwich structures.

3.2. I/V curves with regular current steps: Coulomb staircases

For LB films consisting of four to six monolayers of PcPd, PTCDI-SC5 or PolC5F a considerable fraction of the I/V characteristics exhibited at least one steplike current increase.

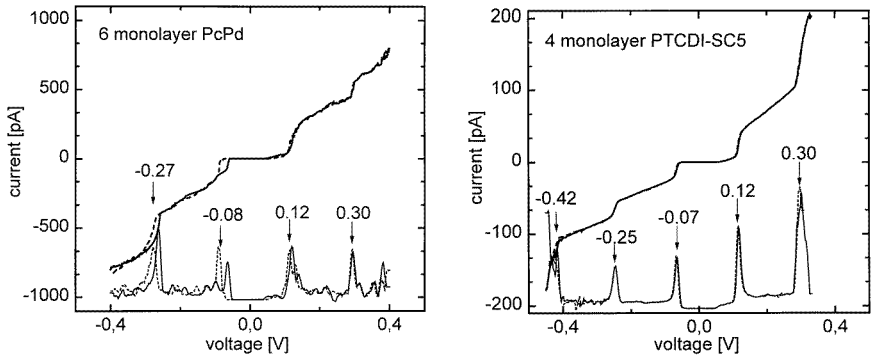

(a) (b)

Figure 3. I/V characteristics at 4.2 K of a sandwich structure consisting of (a, top) six monolayers PcPd, and (b, bottom) four monolayers PTCDI-SC5. In each case, the first scan corresponds to the full line, the second scan to the broken line. The peaks in the first derivative highlight the step positions.

More interestingly, in a few per cent of the LB sandwiches, on which we will focus in the following, *regular* current steps were observed. As representative example for each of the two π-conjugated films at 4.2 K, figure 3(a) shows a staircase-like I/V characteristic obtained from six monolayers of PcPd, while figure 3(b) displays I/V curves measured on a four-monolayer PTCDI-SC5 LB film. In each case, the full line corresponds to the first, the broken line to the second voltage sweep. A bias larger than ± 0.5 V was not applied because at these values current fluctuations started to become significant.

In the curves of figure 3(a), two current steps are observed for negative and positive bias, respectively. From the peak positions in the first derivative, it follows that the steps are almost equidistant with an average separation of about 0.19 V. The change observed between the first and second scan is representative for the low stability observed in general for the PcPd films. In comparison, the PTCDI-SC5 contacts turned out to be somewhat more stable. This is apparent from figure 3(b) which shows a negligible difference between the first and second voltage sweep. The increased stability of the PTCDI-SC5 sandwich junctions upon repeated measurement is attributed to a structural stabilization through interaction [30] between the gold atoms of the top electrode and the sulphur groups in the periphery of the PTCDI-SC5 molecules. The series of five well pronounced, distinct steps is characterized by an average separation of 0.18 V. It should be noted that the period of the steps is just accidentally almost identical to that in figure 3(a) (PcPd LB film). The other PcPd and PTCDI-SC5 sandwich structures with regular steps in the I/V curve were characterized by different, smaller separations.

Compared to the junctions comprising the π-conjugated molecules, some of the PolC5F sandwich structures displayed a very regular staircase over a larger bias range of up to ± 1 V, as demonstrated by figure 4 for a four-monolayer PolC5F LB film at 4.2 K. The high stability of this film is reflected by the identical curves obtained in the first and second voltage scan. The separation of the six well pronounced steps is 0.33 V. Noteworthy, in our experiments with different PolC5F contacts, a step period of maximally 0.35 V was observed. In the range of ± 1 V, an almost linear tunnelling current is observed between the steps. The only indications of the beginning of non-linear transport behaviour are the somewhat larger current steps at -0.84 V and +0.80 V as compared to the steps positioned at -0.51 V, -0.18 V, +0.15 V, and +0.48 V. This broad voltage range compared to the one observed for the π-conjugated molecular films reflects the large barrier height for σ-saturated alkyl chains, which was determined to be about 4.5 eV by Boulas *et al* [31].

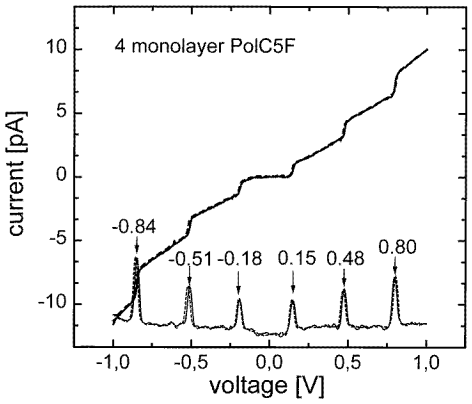

Figure 4. I/V curve of a four-monolayer PolC5F sandwich structure at 4.2 K (full line: first scan, broken line: second scan).

An important question arises concerning the origin of the current steps in the I/V curves of figures 3 and 4. The regular steplike characteristics strongly resemble Coulomb staircases obtained from STM measurements on individual metallic islands [32]. Moreover, the step separation of 0.35 V observed for the PolC5F sandwich junction is close to the value of 0.38 V recently found [33] by Desmicht *et al* in point-contact measurements on cobalt clusters with a diameter of about 2 nm.

In general, a Coulomb staircase is observable for an ultrasmall conducting island in an asymmetric series configuration of two tunnel junctions. This requires that the tunnel resistance R and capacitance C of the two junctions are different, one possibility being $R_1 \ll R_2$ and $C_1 \ll C_2$. For that case [34], the steps are predicted to appear with a period of e/C_2 at voltages of $(2n+1)e/C_2$ (n: integer), and the step height is expected to be $e/[C_2R_2]$.

Support for the assumption that Coulomb charging effects are responsible for the current steps is obtained from numerical simulations of the I/V characteristics. Towards this end, I/V curves obtained with the four-monolayer PolC5F sandwich structure (compare figure 4) were fitted on the basis of the Coulomb blockade model described by Hanna and Tinkham [35]. The corresponding equivalent circuit of an island coupled via two tunnelling barriers to the electrodes is displayed in figure 5. Nature and origin of the island need not be specified for the fits performed in the following. R_1, C_1 and R_2, C_2 represent the resistance and capacitance attributed to the tunnelling barrier close to the top (index 1) and bottom (index 2) electrode, respectively. An important feature of the I/V characteristic in figure 4 is the non-zero current for negative voltages within the gap around zero bias. Such a type of current increase, together with the inherent asymmetry of the curve, are a signature of offset charge effects [36]. These effects can be related to the presence of charges trapped at neighbouring defects, resulting in a shift of the electrostatic potential of the island. This shift is reflected by a finite value of the offset charge Q_0. In contrast to the π-conjugated compounds, sandwich structures composed of the polymer PolC5F exhibited a sufficient stability to perform temperature dependent measurements. Curves fitted (broken lines) to the I/V characteristics (full lines) at three different temperatures (4 K, 50 K and 100 K) are collectively displayed in figure 6. Good agreement between the experimental and simulated curves was achieved with the following fit parameters: $C_1 = 8.0 \times 10^{-19}$ F, $C_2 = 5.0 \times 10^{-19}$ F, $R_1 = 2.0 \times 10^9\ \Omega$, $R_2 = 1.2 \times 10^{11}\ \Omega$, $Q_0 = -0.05e$. Obviously, the inclusion of a non-zero value for Q_0 allows an adequate

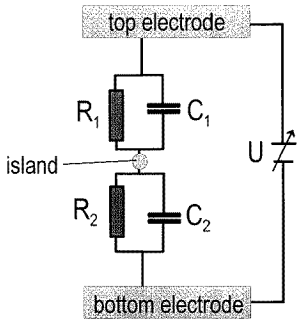

Figure 5. Equivalent circuit for a conducting island embedded in an organic film between top and bottom electrode. C_1, C_2 represent the capacitance over the two tunnelling barriers, respectively. R_1, R_2 are the corresponding tunnel resistances.

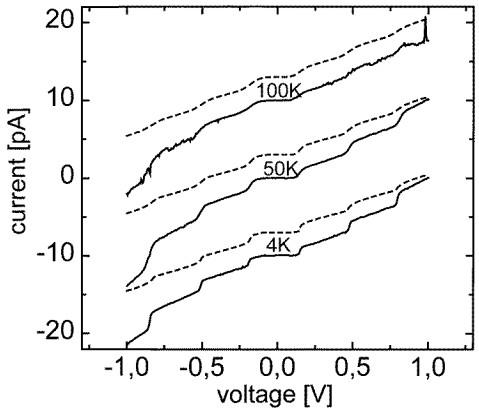

Figure 6. I/V curves (full line) of the four-monolayer PolC5F sandwich at 4 K, 50 K and 100 K with fitted curves (broken line). For clarity, the sets at 4 K and 100 K and the calculated curve at 50 K were offset.

simulation of the experimental data. However, especially for the curves at 50 K and 100 K a significant non-linear current contribution is observed for a bias exceeding about ± 0.4 V, and it is noticed that even in the 4 K characteristic this effect is not fully absent. To shine more light on the origin of these thermally induced irregularities in the staircase, transport measurements were performed over a larger temperature range. The grey scale plot in figure 7 illustrates the temperature dependence of the differential conductance $\mathrm{d}J/\mathrm{d}U$ between 4 K and 200 K. No change in the I/V characteristic could be detected for this contact after it was cooled back again to 4 K. At about 80 K, the steps are starting to smear out but can still be recognized up to 150 K. The maximal temperature T_{max} for Coulomb blockade effects to be observable can be estimated from [37] $T_{max} \approx e^2/8k_B C_\Sigma$ which leads in the present case (total capacitance $C_\Sigma = C_1 + C_2 = 1.3 \times 10^{-18}$ F) to a predicted temperature limit of 179 K. From the fact that this value is in fair agreement with the observed vanishing of the steps at about 150 K, it can be concluded that thermally induced charge fluctuations, not structural instabilities or competing transport processes, are the main source for the changes in figure 7.

The I/V characteristics measured in case of the π-conjugated films could also be fitted in good agreement with the Coulomb blockade model. For example, the fit parameters for the four-monolayer PTCDI-SC5 contact (compare figure 3(b)) were determined to be

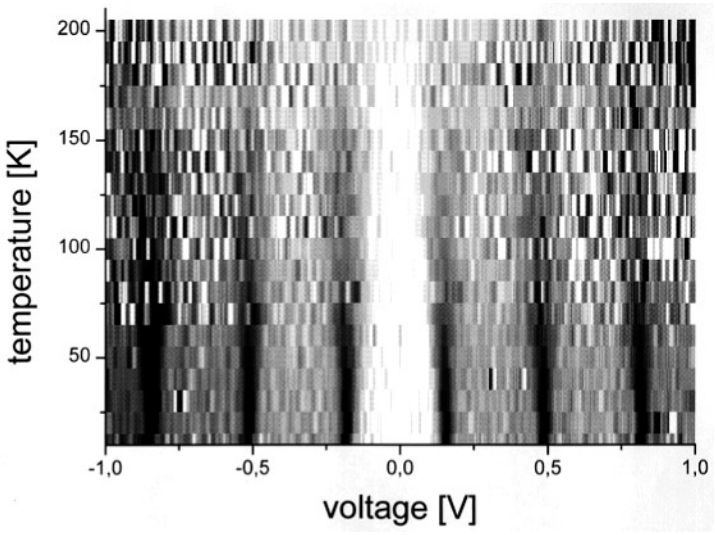

Figure 7. Grey scale plot of differential conductance as a function of temperature and voltage for the four-monolayer PolC5F film.

$C_1 = 9.0 \times 10^{-19}$ F, $C_2 = 9.1 \times 10^{-19}$ F, $R_1 = 5.0 \times 10^7$ Ω, $R_2 = 2.8 \times 10^9$ Ω and $Q_0 = -0.15e$. It is, however, noticed that in the experimental curve the heights of the current steps at −0.4 V and +0.3 V are considerably larger than for the three steps in between (at −0.25 V, −0.07 V and 0.12 V). This observation can be explained by electric field induced suppression of the tunnelling barriers [38], which leads to a transition from a linear to an exponential current dependence. For all Coulomb staircase-like curves found in the case of π-conjugated films ($T = 4.2$ K), the onset of barrier suppression was observed at a bias of maximally ±0.5 V, which is small compared to the voltage range of about ±1 V accessible with inorganic (e.g., Al_2O_3) tunnelling barriers [39]. This result is ascribed to an energy difference of less than about 1 eV between the Fermi level (E_F) of the gold contacts and the HOMO or LUMO of the π system. As a representative example, Hirose *et al* determined the energy barrier between E_F of gold and the LUMO of PTCDA, the parent compound of PTCDI-SC5, to be about 0.5 eV [40]. On the other hand, the barrier height for Al/Al_2O_3 is considerably larger, i.e., in the range of 2.0–2.5 eV [41].

In view of both the similarity between our I/V data and results from tunnelling experiments on metal clusters, and the successful simulation of the staircase-like I/V characteristics in the frame of Coulomb blockade, we assume that the island charged with single electrons consists of a small gold particle. For the three types of LB film, it is proposed that the particles are formed by diffusion of gold atoms into the organic film during thermal evaporation of the top contact. For a rough estimation of the size of the island being charged with single electrons, responsible for the current steps in figure 3(b) (four monolayers PTCDI-SC5), we use the spherical capacitor model for a metallic sphere with radius r surrounded by a larger sphere of radius R. This model is chosen instead of just calculating the self-capacitance of a sphere in an infinite medium in order to account for the capacitance increase due to the presence of the metal electrodes. Thus, with the values of $C_\Sigma = C_1 + C_2 = 1.8 \times 10^{-18}$ F, $2R \approx 7$ nm as thickness of the four-monolayer PTCDI-SC5 film and taking $\varepsilon_r = 3$ as the permittivity of the organic film [42], the size is approximated from $C_\Sigma = 4\pi\varepsilon_0\varepsilon_r/(1/r - 1/R)$ to be $d = 2r = 4.2$ nm. Following the same assumptions

for the four-monolayer PolC5F sandwich structure (figure 4), one estimates the island size $d = 2r$ from the total capacitance $C_\Sigma = 1.3 \times 10^{-18}$ F $= 4\pi\varepsilon_0\varepsilon_r/(1/r - 1/R)$ and using $2R \approx 7.1$ nm to be $d = 3.6$ nm.

That charging of gold particles is the origin of the observed current steps could be supported by recent cross-sectional TEM investigations on (gold/ten-monolayer PolC5F LB film/gold) sandwich structures [43] which indicated the presence of metal particles ($d = 1$–6 nm) located close to the top electrode. Importantly, the island size of 3.6 nm, estimated above by using the total capacitance obtained from the curve fit, falls into the range observed by TEM. The nanometre sized islands might be stabilized through interaction of the particle surface with the π electrons of PcPd or PTCDI-SC5. In case of PTCDI-SC5 and PolC5F, an even stronger interaction is expected with sulphur atoms [44], either being part of the side chains (PTCDI-SC5) or present as free thiol groups–SH (PolC5F/cysteamine). Regarding the low mechanical stability of the organic films and the high diffusion coefficient of noble metals in organic materials [45], we assume that the thickness of the sandwich structures varies locally and, as a consequence, the transport behaviour is dominated by tunnelling through the thinnest part of the contact. If the assumption of such a dominating transport channel is justified, only a small fraction of the present molecules will be involved as tunnelling barriers between the gold island and the electrodes. In addition, a filament originating from diffusion of gold atoms of the top electrode could perform a similar function as the STM tip in the above cited experiments. It is noteworthy that the formation of filaments has also been documented for inorganic devices with oxide tunnelling barriers [46].

4. Summary

A part of the I/V characteristics of sandwich structures composed of a few organic monolayers between two gold electrodes exhibited a pronounced step-like behaviour at low temperatures. In case of the polymer PolC5F films, the stepped I/V curves extended over a voltage range of up to ± 1 V and the current steps persisted up to about 150 K. In contrast, sandwich structures incorporating the π-conjugated molecules PcPd and PTCDI-SC5 were not sufficiently stable to allow temperature dependent measurements. In addition, the transition from a linear to an exponential dependence of the tunnelling current, which is ascribed to barrier suppression, was found to set in at lower voltages than for the PolC5F films. These observations are accounted for by the higher mechanical or thermal stability of PolC5F as well as a larger tunnel barrier height as compared to the π-systems. Single electron tunnelling is considered as origin of the regular steps in the I/V curves. The I/V staircases are attributed to charging of gold islands with sizes in the nanometre range, formed by diffusion of gold atoms from the top gold electrode during evaporation. The presence of these islands and their asymmetric location between the top and bottom electrode, a necessary condition for the observation of a Coulomb staircase, were supported by TEM investigations [43]. The clear single period of the steps in the staircases strongly points to the charging of a *single* gold particle, which might be part of a predominating transport path.

Acknowledgments

Financial support from Sonderforschungsbereich 329 (Molekulare Elektronik) is gratefully acknowledged. The authors appreciate M Hanack and P Haisch for supplying the phthalocyanine derivative PcPd.

References

[1] Bezryadin A, Dekker C and Schmid G 1997 *Appl. Phys. Lett.* **71** 1273
[2] Klein D L, McEuen P L, Bowen Katari J E, Roth R and Alivisatos A P 1996 *Appl. Phys. Lett.* **68** 2574
[3] Zhou C, Deshpande M R, Reed M A, Jones L II and Tour J M 1997 *Appl. Phys. Lett.* **71** 611
[4] Tewordt M, Law V J, Nicholls J T, Martin-Moreno L, Ritchie D A, Kelly M J, Pepper M, Frost J E F, Newbury R and Jones G A C 1994 *Solid-State Electron.* **37** 793
[5] Grabert H and Devoret M (eds) 1992 *Single Charge Tunneling* (New York: Plenum)
[6] Devoret M H, Esteve D and Urbina C 1992 *Nature* **360** 547
[7] Wilkins R, Ben-Jacob E and Jaklevic R C 1989 *Phys. Rev. Lett.* **63** 801
[8] Schönenberger C, van Houten H, Donkersloot H C, van der Putten A M T and Fokkink L G J 1992 *Phys. Scr.* T **45** 289
[9] van Kempen H, Dubois J G A, Gerritsen J W and Schmid G 1995 *Physica* B **204** 51
[10] Schönenberger C, van Houten H and Donkersloot H C 1992 *Europhys. Lett.* **20** 249
[11] Dubois J G A, Gerritsen J W, Shafranjuk S E, Boon E J G, Schmid G and van Kempen H 1996 *Europhys. Lett.* **33** 279
[12] Erokhin V, Facci P, Carrara S and Nicolini C 1995 *J. Phys. D: Appl. Phys.* **28** 2534
[13] Porath D and Millo O 1997 *J. Appl. Phys.* **81** 2241
[14] Sato T and Ahmed H 1997 *Appl. Phys. Lett.* **70** 2579
[15] Klein D L, Roth R, Lim A K L, Alivisatos A P and McEuen P L 1997 *Nature* **389** 699
[16] Burghard M, Fischer C M, Schmelzer M, Roth S, Hanack M and Göpel W 1995 *Chem. Mater.* **7** 2104
[17] Winter C S, Tredgold R H, Vickers A J, Khoshdel E and Hodge P 1985 *Thin Solid Films* **134** 49
[18] Burghard M, Schmelzer M, Roth S, Haisch P and Hanack M 1994 *Langmuir* **10** 4265
[19] Roth S, Blumentritt S, Burghard M, Fischer C M, Philipp G and Mueller-Schwanneke C 1997 *Synth. Met.* **86** 2415
[20] Fischer C M, Burghard M, Roth S and von Klitzing K 1995 *Appl. Phys. Lett.* **66** 3331
[21] Roth S, Burghard M and Fischer C M 1997 *Molecular Electronics* ed J Jortner and M Ratner (Malden: Blackwell) p 255
[22] Giannini C, Tapfer L, Sauvage-Simkin M, Garreau Y, Jedrecy N, Véron M B, Pinchaux R, Burghard M and Roth S 1996 *Thin Solid Films* **288** 272
[23] Fischer C M, Burghard M, Roth S and von Klitzing K 1996 *Surf. Sci.* **361/362** 905
[24] Iwamoto M, Kubota T and Sekine M 1990 *J. Phys. D: Appl. Phys.* **23** 575
[25] Isono Y and Nakano H 1994 *J. Appl. Phys.* **75** 4557
[26] Iwamoto M and Shidoh S 1990 *Japan. J. Appl. Phys.* **29** 2031
[27] Tredgold R H, Vickers A J and Allen R A 1984 *J. Phys. D: Appl. Phys.* **17** L5
[28] Martin A S and Sambles J R 1995 *Thin Solid Films* **260** 222
[29] Movaghar B 1990 *Chem. Phys.* **146** 389
[30] Herdt G and Czandera A W 1994 *J. Vac. Sci. Technol.* A **12** 2410
[31] Boulas C, Davidovits J V, Rondelez F and Vuillaume D 1996 *Phys. Rev. Lett.* **76**
[32] Amman M, Wilkins R, Ben-Jacob E, Maker P D and Jaklevic R C 1991 *Phys. Rev.* B **43** 1146
[33] Desmicht R, Faini G, Cros Y, Fert A, Petroff F and Vaurès A 1998 *Appl. Phys. Lett.* **72** 386
[34] Mullen K, Ben-Jacob E, Jaklevic R C and Schuss Z 1988 *Phys. Rev.* B **37** 98
[35] Hanna A E and Tinkham M 1991 *Phys. Rev.* B **44** 5919
[36] Dubois J G A, Verheijen E N G, Gerritsen J W and van Kempen H 1993 *Phys. Rev.* B **48** 11 260
[37] Altmeyer S, Kühnel F, Spannenberg B and Kurz H 1996 *Semicond. Sci. Technol.* **11** 1502
[38] Korotkov A and Nazarov Y 1991 *Physica* B **173** 217
[39] Kreupl F, Vancea J, Risch L, Hofmann F and Hoffmann H 1996 *Microelectron. Eng.* **30** 451
[40] Hirose Y, Kahn A, Aristov V, Soukiassian P, Bulovic V and Forrest S R 1996 *Phys. Rev.* B **54** 13 748
[41] Altmeyer S, Spangenberg B and Kurz H 1995 *Appl. Phys. Lett.* **67** 569
[42] *CRC Handbook of Chemistry and Physics* 1987 (Boca Raton, FL: Chemical Rubber Company)
[43] Philipp G, Mueller-Schwanneke C, Burghard M and Roth S 1999 *J. Appl. Phys.* **85**
[44] Ulman A 1991 *Introduction to Ultrathin Organic Films* (San Diego: Academic)
[45] Couch N R, Movaghar B and Girling J R 1986 *Solid State Commun.* **59** 7
[46] Wiesendanger R 1994 *Scanning Probe Microscopy and Spectroscopy* (Cambridge: Cambridge University Press) ch 1